Application of adiabaticity map

highly efficient coupling from optical fibers to silicon waveguides by adiabatic mode evolution

Chang, Li Fu; Norte, Richard; Westerveld, Wouter J.; Tseng, Shuo Yen

DOI
10.1117/12.2692415

Publication date
2023

Document Version
Final published version

Published in
Emerging Applications in Silicon Photonics IV

PROCEEDINGS OF SPIE

SPIEDigitalLibrary.org/conference-proceedings-of-spie

Application of adiabaticity map: highly efficient coupling from optical fibers to silicon waveguides by adiabatic mode evolution

Li-Fu Chang, Richard Norte, Wouter Westerveld, Shuo-Yen Tseng

Li-Fu Chang, Richard Norte, Wouter J. Westerveld, Shuo-Yen Tseng, "Application of adiabaticity map: highly efficient coupling from optical fibers to silicon waveguides by adiabatic mode evolution," Proc. SPIE 12794, Emerging Applications in Silicon Photonics IV, 127940B (30 November 2023); doi: 10.1117/12.2692415

SPIE.

Event: SPIE Photonex, 2023, Glasgow, United Kingdom

Application of adiabaticity map: highly efficient coupling from optical fibers to silicon waveguides by adiabatic mode evolution

Li-Fu Chang[a], Richard Norte[b], Wouter J. Westerveld[b], and Shuo-Yen Tseng[a]

[a]Department of Photonics, National Cheng Kung University, No. 1 University Rd., Tainan 701, Taiwan

[b]Department of Precision and Microsystems Engineering, Delft University of Technology, 2628 CD Delft, The Netherlands

ABSTRACT

Efficient coupling of light from an optical fiber to silicon waveguides is a challenging task in integrated photonics. Couplers based on adiabatic mode evolution have the advantages of high bandwidth and low loss but are often accompanied by longer device lengths. In this paper, we introduce the concept of adiabaticity map and optimize the coupling between an optical fiber and Si waveguides by selecting routes on the map that minimize unwanted mode coupling. The map clearly indicates areas in mode evolution where supermode coupling is large and identifies optimal routes for efficient mode evolution. Optimized interaction length and widths are obtained from the adiabaticity map. We obtain highly efficient coupling (96%) with large bandwidth (1-dB bandwidth 280 nm) and misalignment tolerance (>90 nm lateral misalignment range for 1-dB excess losses) for the TE polarization.

Keywords: Coupler, silicon photonics, mode evolution, adiabatic

1. INTRODUCTION

Optical interconnection between photonic chips and optical fibers is frequently utilized throughout the entire photonic integrated circuit (PIC) system. Therefore, efficient fiber-to-chip coupling is an important issue that requires attention.[1] The main challenge is the significant size mismatch between the fundamental modes of optical fibers and the optical modes of PIC waveguides. While the silicon-on-insulator (SOI) platform provides tight optical confinement, enabling the integration of numerous devices on a single chip, the small size also gives rise to other issues. The standard single-mode fiber has a diameter of 125 μm, with a core diameter of about 9 μm. In contrast, the single-mode silicon waveguide based on SOI is composed of high refractive index silicon and low refractive index silicon dioxide, resulting in a higher refractive index contrast that concentrates the optical field. The size of the single mode silicon (Si) waveguide is about 400(W) $\times$220(H) nm^2.

In contrast to conventional edge couplers which apply butt coupling or end-fire coupling,[2] a new coupling approach based on adiabatic mode evolution between the optical fiber and the Si waveguide[3] is considered in this work, as illustrated in Fig. 1(a)(b)(c). We consider a optical fiber taper (OFT) prepared by wet etching techniques with a taper angle of 1.5° and $R_1 = 1\mu$m.[4] The HE_{11} fiber mode can adiabatically evolve over the entire length of the OFT ($\sim$150 μm long). To avoid leakage into the buried oxide (BOX) layer, which has a similar refractive index to that of the optical fiber, the Si waveguide structure is suspended over the coupling region. The Si waveguide is linearly tapered from W_G =400 nm to W_1 =40 nm. The coupling structure consists of two oppositely tapered waveguides overlapped spatially with each other with an overlapping length of L. The coupling region of length L is defined by the widths of the Si waveguide at the start (W_2) and the end (W_1)of the overlap area [Fig. 1(c)].

In Fig. 1(d), we show the supermodes of the coupler along the coupling region by assuming $W_1 = 40$ nm and $W_2 = 400$ nm. When the adiabaticity criterion is satisfied, the HE_{11} fiber mode evolves adiabatically to

Further author information: (Send correspondence to S.-Y.T.)

S.-Y.T.: E-mail: tsengsy@mail.ncku.edu.tw

Emerging Applications in Silicon Photonics IV, edited by Callum G. Littlejohns, Marc Sorel, Proc. of SPIE Vol. 12794, 127940B · © 2023 SPIE
0277-786X · doi: 10.1117/12.2692415

the TE_{00} mode of the Si waveguide evolving along supermode 1, achieving high efficiency and large bandwidth coupling. The key is to minimize coupling to supermode 3 during mode evolution. The coupling efficiency (CE) is thus a function of the interaction length and coupling region geometry, which is determined by the Si waveguide parameters. In this paper, we analyze the adiabaticity of the coupling region using the adiabaticity map, which reveals regions in the parameter space where non-adiabatic coupling is strong. The coupling structure can then be optimized by designing evolution paths around these non-adiabatic regions, resulting in highly efficient couplers.

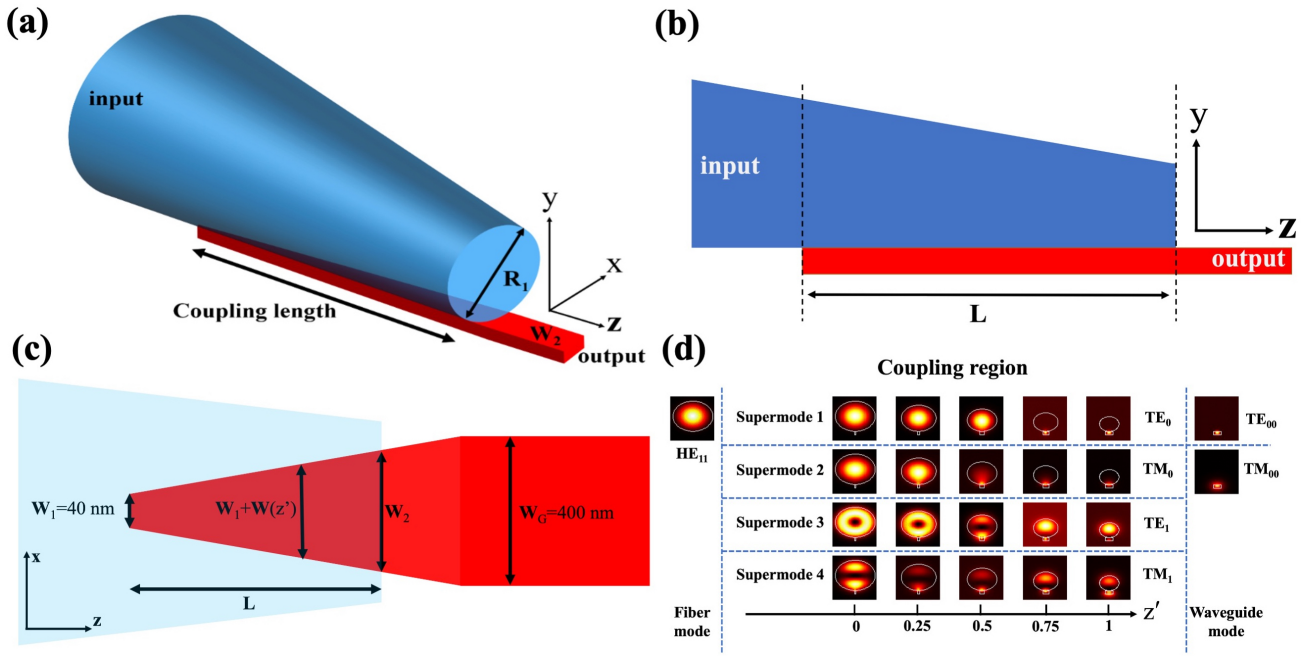

Figure 1. (a) 3-D Schematic of the optical fiber to Si waveguide coupler based on mode evolution. (b) Side view of the coupler. (c) Top view of the coupler. (d) Supermodes of the coupler along the coupling region.

2. ADIABATICITY MAP

In photonics, the adiabatic condition describes a process in which the variation of optical modes in the propagation direction (z-axis) occurs slowly enough so that light remains in the same eigenmode throughout the entire propagation process.[5] We define the adiabaticity parameter c as:[6]

$$c(z) = \left| \frac{\langle m| \frac{d}{dz} |n\rangle}{\beta_m - \beta_n} \right|, \tag{1}$$

where $|m, n\rangle$ are the supermodes of the coupling region, and $\beta_{m,n}$ are the propagation constants of the eigenmodes. The adiabaticity parameter indicates the strength of unwanted coupling between eigenmodes m and n.

The coupler in this work involves the OFT and the Si waveguide. In the coupling region, two spatial parameters need to be considered, namely, the OFT diameter R and the silicon waveguide width variation W. Firstly, the eigenmodes of the local cross section in the coupling region are determined, and the local supermodes are calculated as shown in Fig. 1(d). Subsequently, the instantaneous adiabaticity parameters are computed by Eq. (1) using supermodes 1 and 3. Finally, the adiabaticity parameter is represented on a map as a function of W and R. Fig. 2 shows the adiabaticity map, where the horizontal axis represents the variation of the Si waveguide width, and the vertical axis represents the core diameter of OFT. This map enables the observation of the distribution of adiabaticity parameters along different evolution paths.

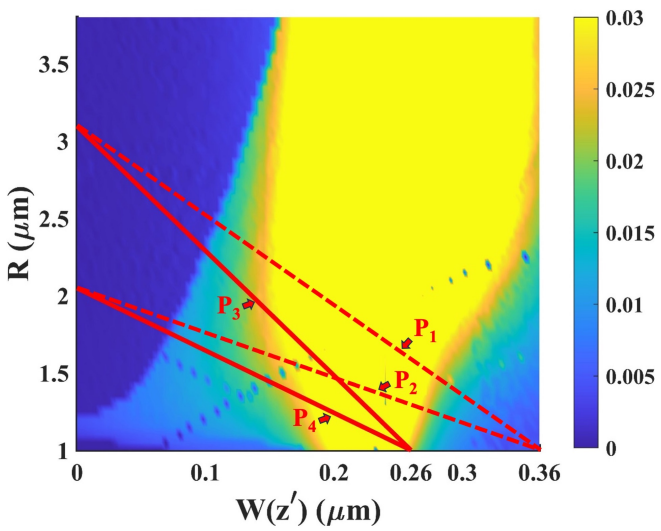

Figure 2. Adiabaticity map showing adiabaticity parameter in the coupling region. P_1, P_2, P_3, and P_4 are different evolution paths.

3. OPTIMIZATION OF THE COUPLING REGION

Intuitively, one would design the coupling region such that the end of the OFT coincide with the start of the waveguide taper, that is $W_2 = W_G = 400$ nm. In this case, one would also expect that a longer coupling length should result in a higher CE due to more adiabatic mode evolution. In Fig. 3(a), we show the calculated CE from the HE_{11} fiber mode to the TE_{00} mode of the Si waveguide as a function of L. It can be seen that the CE reaches ∼70% when L is between 20 and 40 μm, and then steadily decreases with longer L. To explain this phenomenon, we draw two paths P_1 and P_2 on the adiabaticity map, Fig. 2, corresponding to coupling lengths of L=40 and 20 μm in Fig. 3(a), respectively. Clearly, these two paths cross regions where the supermode coupling is large on the map, with P_1 seeing more unwanted coupling than P_2. Therefore, even at a longer length, P_1 only achieves a similar CE as P_2. Also, we can see that as long as W_2=400 nm [$W(z') = 0.36\mu$m], any path corresponding to longer L on the map will always cross the region where unwanted coupling is large, thus explaining the decreasing CE with L.

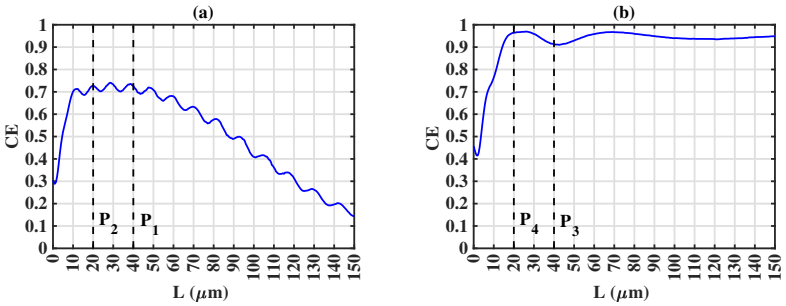

Figure 3. Coupling efficiency (CE) as a function of the coupling region length L. (a) Original design with $W_2 = 400$ nm. (b) Optimized design with $W_2 = 300$ nm. P_1 through P_4 are mode evolution paths corresponding to the paths in Fig. 2.

From the map, we can optimize the mode evolution path. By choosing W_2=300 nm [$W(z') = 0.26\mu$m], we can see from Fig. 1(d) that supermode 1 is sufficiently close to the Si waveguide TE_{00} mode. Now, the evolution paths P_3 and P_4 in Fig. 2, corresponding to L=40 and 20 μm, no longer see the large supermode coupling along P_1 and P_2. The calculated CE as a function of L with the optimized coupling region is shown in Fig. 3(b). We observe that at lengths larger than 15 μm, the CE is steadily larger than 90%. At L=20 μm, a large CE of 96%

can be obtained. Simply by moving the tip of the fiber from W_2=400 nm to W_2=300 nm, we can optimize the coupling region and increase the CE by 25%.

4. BANDWIDTH AND TOLERANCE

Fig. 4(a) shows the device bandwidth for the optimized coupler with $L = 20$ μm and $W_2 = 300$ μm, where the 1-dB bandwidth ranges from 1.43 μm to 1.71 μm, a width of approximately 280 nm; and the 3-dB bandwidth ranges from 1.3 μm to 1.9 μm, a width of approximately 600 nm, with a center operating wavelength of 1.55 μm. The fabrication tolerance is simulated by changing the overall width of the Si waveguide by an amount ΔW. The results are shown in Fig. 4(b), where 1-dB loss can be maintained for ΔW ranges from -28 nm to 59nm.

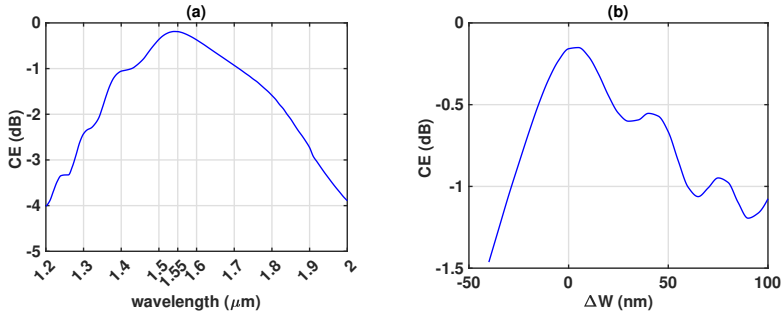

Figure 4. Coupling efficiency (CE) as a function of (a) wavelength and (b) Si waveguide width variation.

Considering the alignment tolerance of the OFT, Fig 5(a) shows the alignment tolerance in the y-direction of the coupling region, which refers to whether the fiber is in close proximity of the silicon waveguide. Within a range of 100nm, the CE loss is smaller than 1-dB; and at 220nm, it reaches 3-dB. Misalignment in the x direction, Δx, disrupts the symmetry of the structure, and it leads to the excitation of undesired modes, resulting in a decrease in CE, as shown in Fig. 5(b). At $\pm$90 nm, the CE loss can be below 1-dB. Since the initial designed coupling length L is 20 μm, a coupling region overlap greater than 20 μm indicates an excessive overlap between the fiber and the waveguide in the z-direction, while a overlap less than 20 μm indicate insufficient overlap. Fig. 5(c) shows the relationship between the overlap length in the coupling region and the CE. It can be observed that for overlap length ranging from 17 μm to 26 μm, the CE loss is smaller than 1-dB, for a range of 14 μm to 33 μm, the CE loss is smaller than 3-dB.

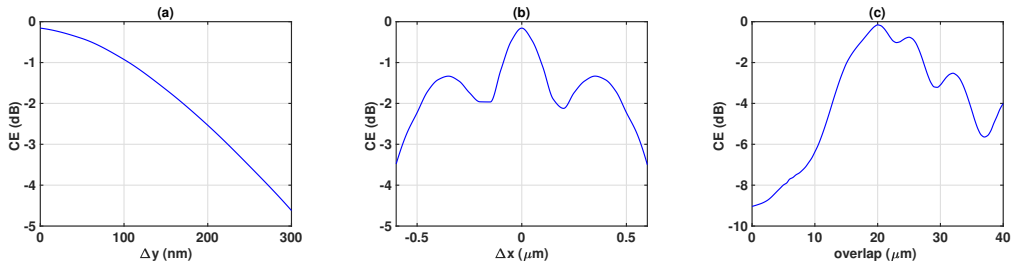

Figure 5. Fiber alignment tolerance in the (a) y-direction, (b) x-direction, and (c) z-direction.

5. CONCLUSION

We present the design and optimization of a mode evolution coupler composed of an OPT and a tapered Si waveguide. The optimization of mode evolution region is achieved using the adiabaticity map, which allows us to identify adiabatic paths for efficient mode evolution. By avoiding high-coupling regions on the map, the mode evolution process in the coupler is optimized, leading to an efficient, compact, and broadband mode evolution coupler. Adiabaticity maps are useful for illustrating the adiabaticity parameter under various device parameter

variations, allowing insights into the adiabatic behavior. This concept can be applied to various devices based on adiabatic mode evolution.

ACKNOWLEDGMENTS

This work is supported in part by the National Science and Technology Council of Taiwan under contracts 111-2221-E-006-052-MY3, 111-2923-B-006-002-MY4, and 112-3111-E-992-001.

REFERENCES

[1] Son, G., Han, S., Park, J., Kwon, K., and Yu, K., "High-efficiency broadband light coupling between optical fibers and photonic integrated circuits," *Nanophotonics* **7**, 1845–1864 (2018).

[2] Marchetti, R., Lacava, C., Carroll, L., Gradkowski, K., and Minzioni, P., "Coupling strategies for silicon photonics integrated chips," *Photonics Res.* **7**, 201–239 (2019).

[3] Son, G., Pradono, R. A., You, J. B., Jeong, Y., Kwon, K., Park, J., Han, S., Han, D. S., Jung, Y., and Yu, K., "Highly efficient broadband adiabatic mode transformation between single-mode fibers and silicon waveguides," *J. Lightw. Technol.* , 1–9 (2023).

[4] Burek, M. J., Meuwly, C., Evans, R. E., Bhaskar, M. K., Sipahigil, A., Meesala, S., Machielse, B., Sukachev, D. D., Nguyen, C. T., Pacheco, J. L., Bielejec, E., Lukin, M. D., and Lončar, M., "Fiber-coupled diamond quantum nanophotonic interface," *Phys. Rev. Appl.* **8**, 024026 (2017).

[5] Sun, X., Liu, H.-C., and Yariv, A., "Adiabaticity criterion and the shortest adiabatic mode transformer in a coupled-waveguide system," *Opt. Lett.* **34**, 280–282 (2009).

[6] Chung, H.-C., Lee, K.-S., and Tseng, S.-Y., "Short and broadband silicon asymmetric y-junction two-mode (de)multiplexer using fast quasiadiabatic dynamics," *Opt. Express* **25**, 13626–13634 (2017).